Supporting Information

Amyloid formation under complicated conditions in which β_2-microglobulin coexists with its proteolytic fragments

Hiroya Muta[‡,1], Masatomo So[‡,1], Kazumasa Sakurai[§,1], Jozsef Kardos[¶], Hironobu Naiki[†], and Yuji Goto[‡,*]

[‡]Institute for Protein Research, Osaka University, Yamadaoka 3-2, Suita, Osaka 565-0871, Japan; [§]Institute of Advanced Technology, Kindai University, Wakayama 649-6493, Japan; [¶]ELTE NAP Neuroimmunology Research Group, Department of Biochemistry Eötvös Loránd University, Pázmány P. sétány 1/C, Budapest, 1117, Hungary; [†]Faculty of Medical Sciences, University of Fukui, Fukui 910-1193, Japan.

Supporting information includes:

SI Text

Table S1

Figures S1-S7

Supporting references

SI Text

Supplementary Results

Cross-seeding Reactions between K3 and β2m. We performed a series of cross-seeding experiments between K3 and β2m monitored with a fluorimeter (Fig. S1). The addition of K3 fibril seeds into the K3 or β2m monomers eliminated the lag time, as previously reported.[1] The addition of β2m fibrils also eliminated the lag time from the spontaneous amyloid formation of β2m or K3 monomers. Elongation kinetics (i.e. the growth rate and maximum values of ThT) depended on the monomer species. CD spectra showed that the secondary structures of amyloid fibrils were also dependent on monomer species. Thus, although K3 or intact β2m seed fibrils may cross-react with β2m or K3 monomers, respectively, seeds cannot define the overall structures of amyloid fibrils. β2m[2, 3] and K3 fibrils[4] appear to have distinct 3D structures, even if β2m amyloid fibrils accommodate K3 amyloid structures.

Supplementary Discussion

Separation of R_2 into Intrinsic and Excess Components. Since a convex smooth R_2 pattern against the sequence is expected for a random coil, as observed for K2, K5, K7, and K9 (Fig. S4), the R_2 profile for K3 at low concentrations of urea with significant deviations from a convex pattern suggested that these deviated residues contributed to residual structures (Fig. S4B). It is assumed that the observed R_2 values ($R_{2,obs}$) comprise two terms, $R_{2,intrin}$ and $R_{2,excess}$:

$$R_{2,obs} = R_{2,intrin} + R_{2,excess} \quad \text{(eq. S1)},$$

where $R_{2,intrin}$ and $R_{2,excess}$ indicate an intrinsic contribution from a random coil and an excess contribution from residual structures with slow chain motion, respectively. There is a semi-empirical equation for the calculation of $R_{2,intrin}$;

$$R_{2,\mathrm{intrin}}(i) = R_{2,\mathrm{residue}} \sum_{j=1}^{N} \exp\left(\frac{|i-j|}{\lambda}\right) + R_{2,\mathrm{SS}} \sum_{k=1}^{N} \exp\left(-\frac{|i-\mathrm{Cys_k}|}{\lambda}\right) \quad \text{(eq. S2)},$$

where $R_{2,\mathrm{residue}}$ and $R_{2,\mathrm{SS}}$ are contributions per residue for residues in the random coil state and linked by a disulfide bond, respectively. λ is the persistent length in the number of residues. $R_{2,\mathrm{excess}}$ indicates the contribution of a residual structure and is assumed to bring an additional contribution with a Gaussian shape to the $R_{2,\mathrm{intrin}}$ pattern.[5] In the present study, since the samples were relatively short peptides, the Gaussian assumption was not appropriate for the analysis. Thus, we manually adjusted the parameters $R_{2,\mathrm{residue}}$, $R_{2,\mathrm{SS}}$, and λ to reproduce $R_{2,\mathrm{obs}}$ for mobile residues (Fig.S4, solid lines, and see Table S1 for the obtained parameter set). We then subtracted $R_{2,\mathrm{intrin}}$ from $R_{2,\mathrm{obs}}$. The remainder was considered to be $R_{2,\mathrm{excess}}$.

Almost nothing remained for non-amyloidogenic peptides (K2, K5, K7, and K9) at any concentrations of urea. On the other hand, K3 showed significant remaining contributions at low urea concentrations (*i.e.*1 and 2 M urea, Fig. S4B, solid lines), representing hydrophobic clusters at low urea concentrations.

Table S1. Parameters used for obtaining an intrinsic contribution according to eq. 3.

	[urea]	Value
Λ	Any	2.5 (residues)
$R_{2,\mathrm{intrin}}$	0 M	0.25~0.28 s^{-1}
	1 M	0.26 s^{-1}
	2 M	0.27 s^{-1}
	4 M	0.29~0.32 s^{-1}
	8 M	0.35~0.41 s^{-1}
$R_{2,\mathrm{SS}}$	8 M	3.0 s^{-1}

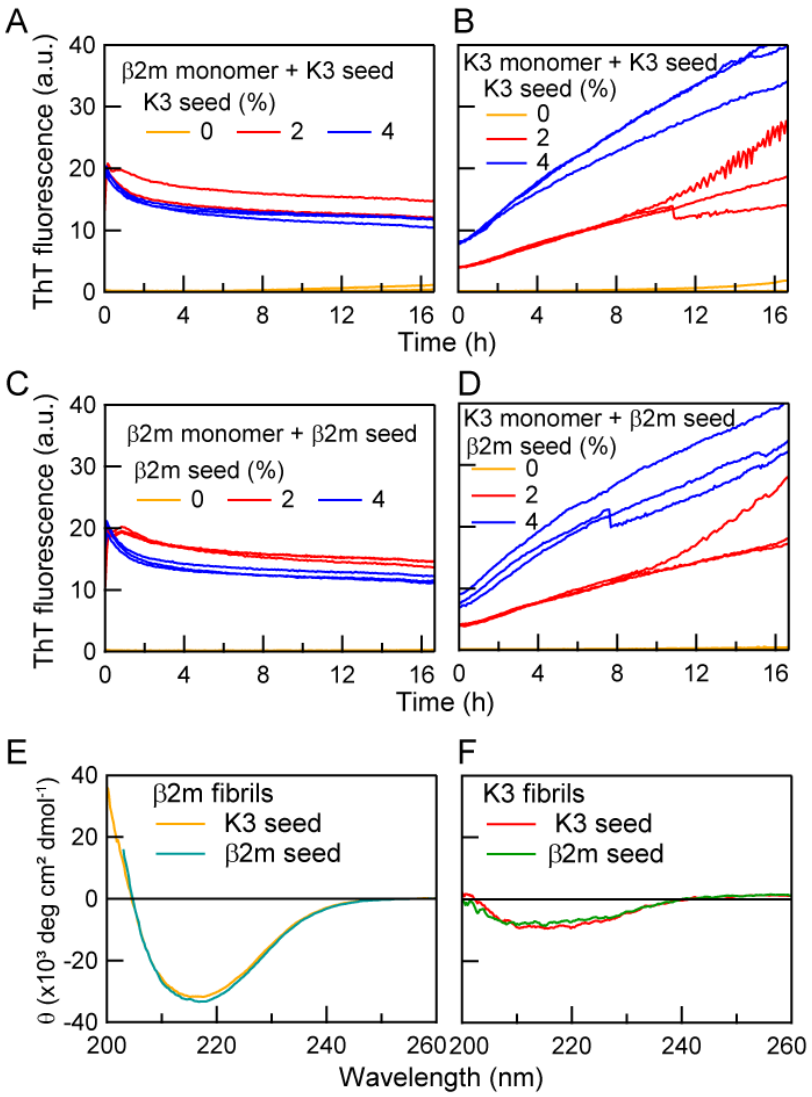

Figure S1. Cross-seeding experiments between K3 and β2m monitored by a microplate reader. (A-D) Real-time observations of seed-dependent amyloid formation followed by ThT fluorescence at 485 nm. The seeds obtained by fibrillation of 25 μM K3 enhanced the subsequent fibrillation of 25 μM K3 (A) and 25 μM β2m (B). The seeds obtained by the fibrillation of 25 μM β2m enhanced subsequent fibrillation in 25 μM β2m (C) and 25 μM K3 (D). CD spectra were categorized into two types: one similar to that of K3 fibrils with a minimum at 215 nm (E) and the other similar to that of β2m fibrils with a minimum at 217 nm (F).

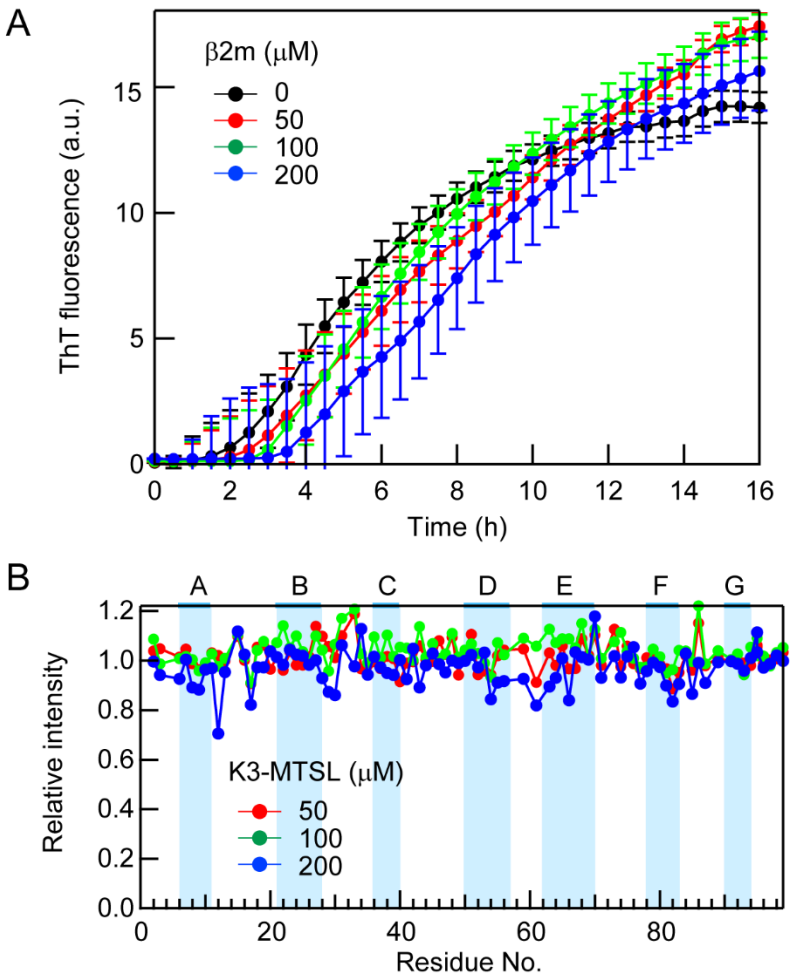

Figure S2. Interaction between K3 and native β2m monitored by PRE measurements at pH 7.0. (A) Kinetics of K3 amyloid formation in the presence of various concentrations of β2m. (B) Profiles of PRE effects for the assigned residues of native β2m at various concentrations of MTSL-labeled K3. The locations of β-strands A-G in the native structure are indicated.

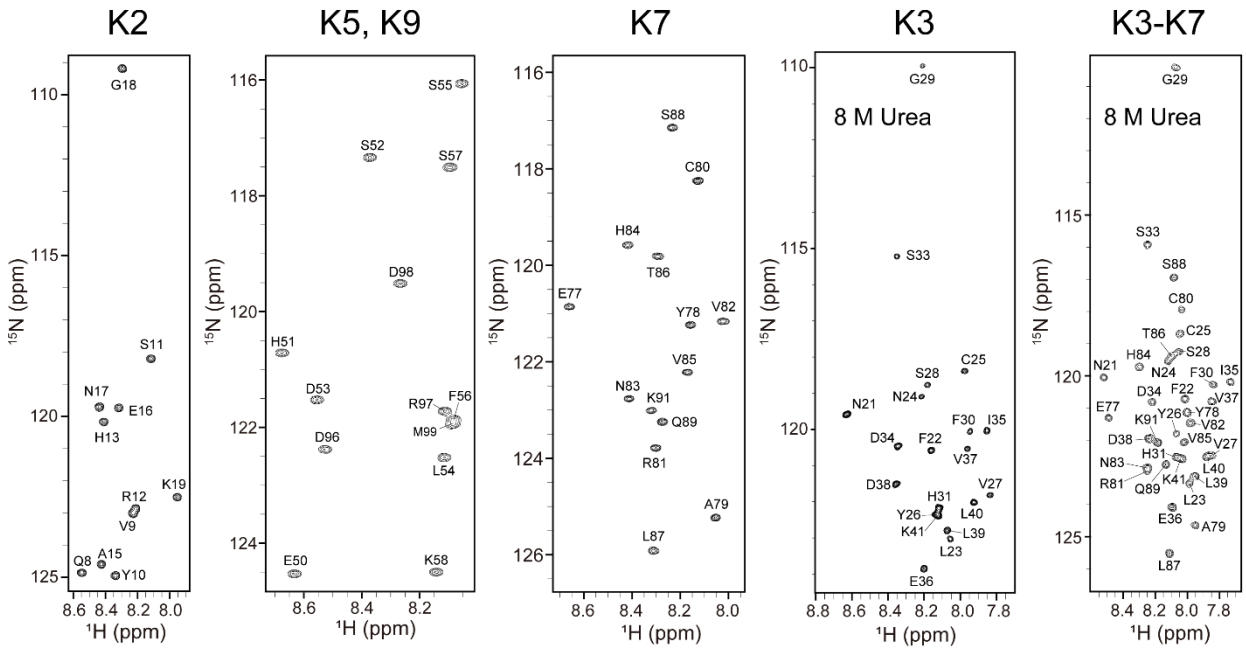

Figure S3. ^{1}H-^{15}N HSQC spectra of isolated proteolytic fragments: (A) K2, (B) K5 and K9, (C) K7, (D) K3, and (E) K3-7. Spectra were obtained in the absence of urea for non-amyloidogenic peptides (K2, K5, K7, and K9) and in 8 M urea for amyloidogenic peptides (K3 and K3-7). Assigned residues are indicated in the spectra.

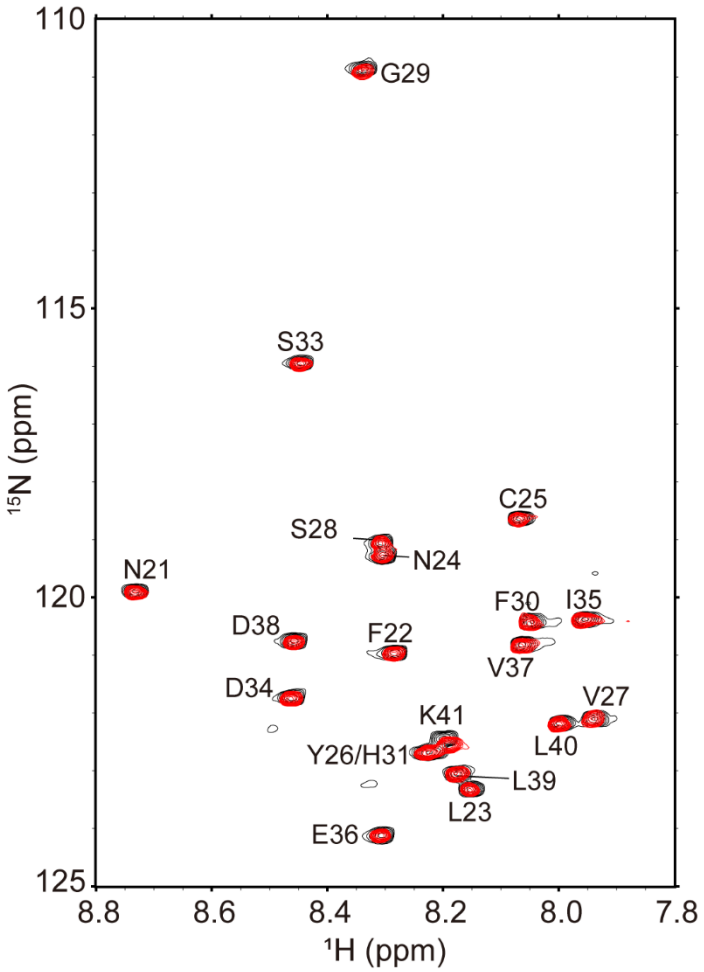

Figure S4. Comparison of ^{1}H-^{15}N HSQC spectra of 50 µM ^{15}N-labelled K3 in the presence (red) and absence (black) of a proteolytic mixture of non-labeled β2m at 75 µM. The spectrum without proteolytic fragments (black) was taken from Fig. 2.

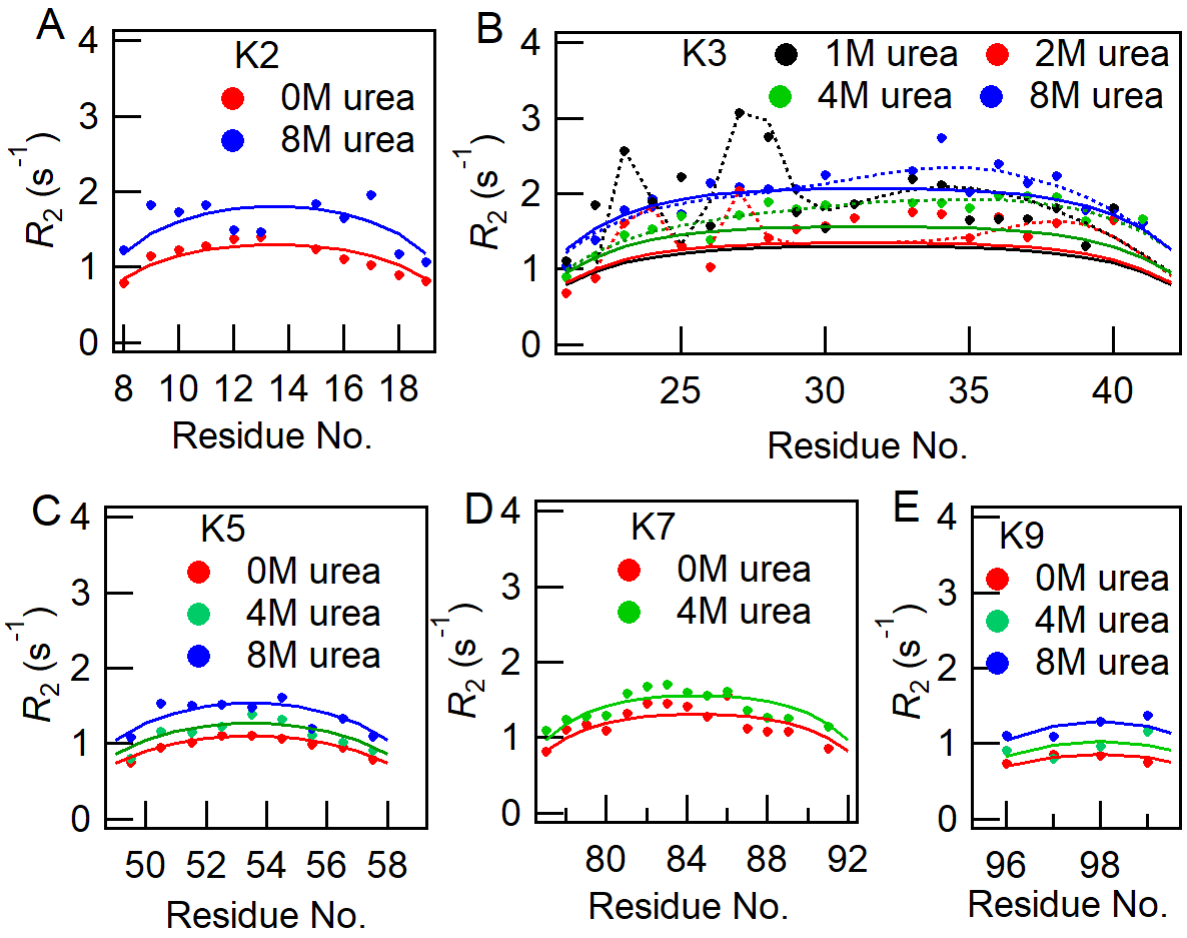

Figure S5. Residue-dependent R_2 values for proteolytic fragments of β2m. (A-E) R_2 values for K2 (A), K3 (B), K5 (C), K7 (D), and K9 (E) measured in the presence of various concentrations of urea. The contributions of the $R_{2,intrin}$ (solid lines) and $R_{2,excess}$ (dotted lines for K3) terms are indicated.

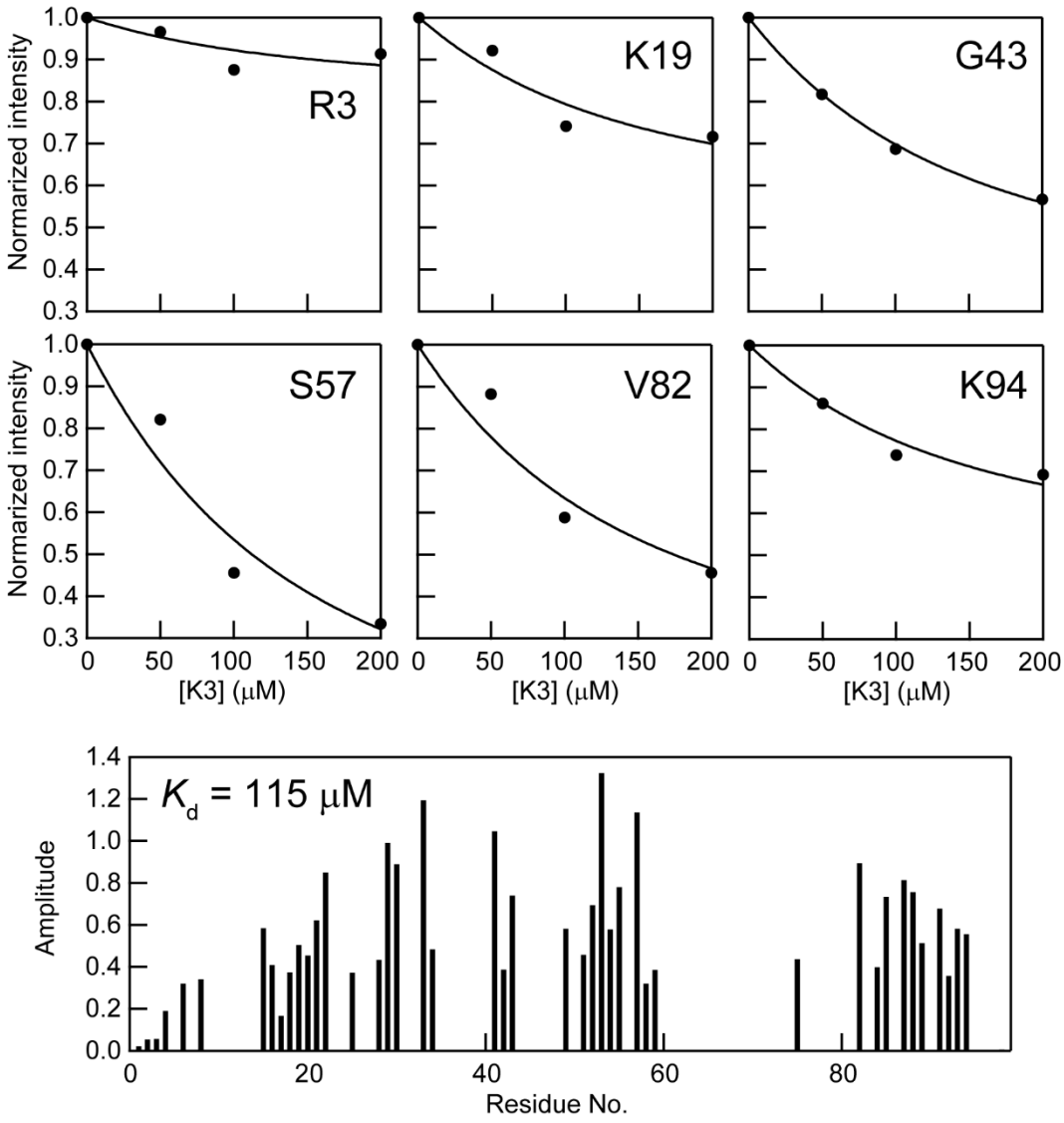

Figure S6. The K_d value calculated from PRE measurement. Intensity decays (circle) and theoretical curves (line) of residue R3, K19, G43, S57, and K94 were plotted using the K_d value of 115 uM. The amplitude of signal decay against residue number was shown (lower panel). The K_d value was calculated by global fitting of the signal decay data assuming one-to-one binding model.

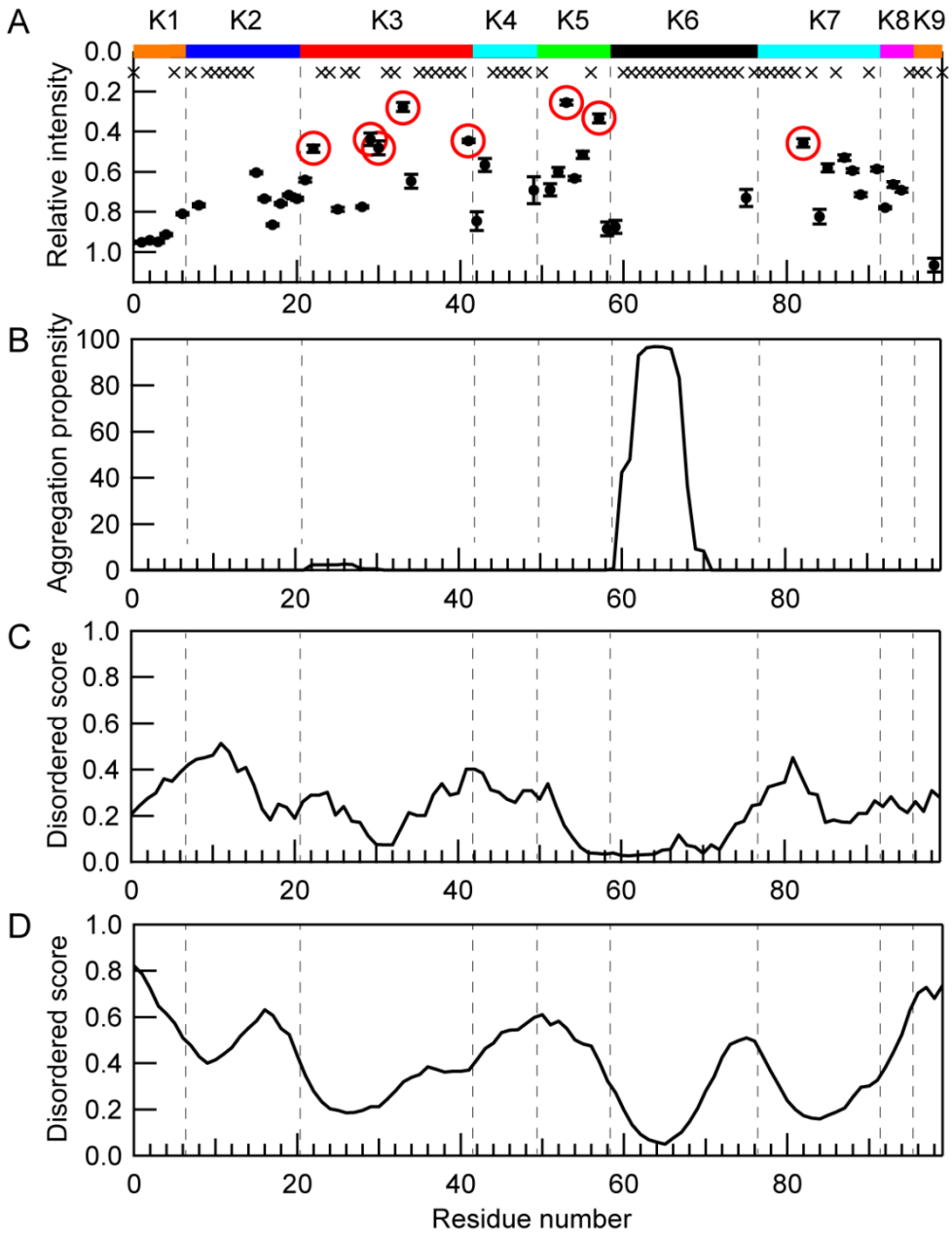

Figure S7. Comparison of various residue-dependent propensities of β2m. (A) The PRE profile at 200 μM K3-MTSL shown in Fig. 3C (same as Figure 6A). (B) Profile of the aggregation propensity calculated by TANGO.[6] (C, D) Profile of the intrinsically disordered regions predicted by IUPred[7] (C) and PONDR[8] (D).

References

(1) Kozhukh, G. V., Hagihara, Y., Kawakami, T., Hasegawa, K., Naiki, H., and Goto, Y. (2002) Investigation of a peptide responsible for amyloid fibril formation of β_2-microglobulin by achromobacter protease I, *J. Biol. Chem. 277*, 1310-1315.

(2) Hoshino, M., Katou, H., Hagihara, Y., Hasegawa, K., Naiki, H., and Goto, Y. (2002) Mapping the core of the β2-microglobulin amyloid fibril by H/D exchange, *Nat. Struct. Biol. 9*, 332-336.

(3) Iadanza, M. G., Silvers, R., Boardman, J., Smith, H. I., Karamanos, T. K., Debelouchina, G. T., Su, Y., Griffin, R. G., Ranson, N. A., and Radford, S. E. (2018) The structure of a β_2-microglobulin fibril suggests a molecular basis for its amyloid polymorphism, *Nat. Commun. 9*, 4517.

(4) Iwata, K., Fujiwara, T., Matsuki, Y., Akutsu, H., Takahashi, S., Naiki, H., and Goto, Y. (2006) 3D structure of amyloid protofilaments of β_2-microglobulin fragment probed by solid-state NMR, *Proc. Natl. Acad. Sci. U. S. A. 103*, 18119-18124.

(5) Platt, G. W., McParland, V. J., Kalverda, A. P., Homans, S. W., and Radford, S. E. (2005) Dynamics in the Unfolded State of β2-microglobulin Studied by NMR, *J. Mol. Biol. 346*, 279-294.

(6) Fernandez-Escamilla, A.-M., Rousseau, F., Schymkowitz, J., and Serrano, L. (2004) Prediction of sequence-dependent and mutational effects on the aggregation of peptides and proteins, *Nat. Biotechnol. 22*, 1302-1306.

(7) Mészáros, B., Erdős, G., and Dosztányi, Z. (2018) IUPred2A: context-dependent prediction of protein disorder as a function of redox state and protein binding, *Nucleic Acids Res. 46*, W329-W337.

(8) Obradovic, Z., Peng, K., Vucetic, S., Radivojac, P., and Dunker, A. K. (2005) Exploiting heterogeneous sequence properties improves prediction of protein disorder, *Proteins 61*, 176-182.